

NUMERICAL PREDICTION OF ENGINEERED WOOD FLOORING DEFORMATION

Pierre Blanchet^{†1}

Research Scientist
Forintek Canada Corp.
319, rue Franquet
Sainte-Foy, Québec, Canada G1P 4R4

Guy Gendron

Professor
Département de génie mécanique
Groupe interdisciplinaire de recherche en éléments finis (GIREF)

Alain Cloutier[†]

Professor
Département des sciences du bois et de la forêt
Groupe interdisciplinaire de recherche en éléments finis (GIREF)

and

Robert Beauregard[†]

Associate Professor
Département des sciences du bois et de la forêt
Centre de recherche sur les Technologies de l'Organisation Réseau (CENTOR)
Université Laval, Québec, Québec, Canada, G1K 7P4

(Received February 2004)

ABSTRACT

Dimensional stability is of primary importance in the use of layered wood composites such as engineered wood flooring. It is largely due to the physical and mechanical properties and moisture content changes of each layer. Therefore, the non-homogeneous adsorption or desorption of moisture by the composite may induce its deformation, thus decreasing product value. The objective of this study was to develop a finite element model of the hygromechanical cupping in layered wood composite flooring. The model is based on two sets of equations: 1) the three-dimensional equations of unsteady-state moisture diffusion, and 2) the three-dimensional equations of elasticity including the orthotropic Hooke's law, which takes into account the shrinkage and swelling of each layer. The proposed model was used to predict the deformation of an engineered wood flooring strip following desorption by the top surface. The model was solved by the finite element method, and the calculated cupping was validated against experimental data. The results show that the proposed model can be successfully used to simulate the non-homogeneous moisture movement and the resulting cupping deformation in layered wood composites such as engineered wood flooring strips. For both predicted and measured deformation, roughly 80% of the cupping deformation appears after 3 days of conditioning. The low water vapor diffusion coefficient of the urea-formaldehyde film used between the surface and core layers of the strip plays a key role in the deformation process. After 42 days of conditioning, the model results overestimated the experimental results by 12% but were within one standard deviation of the experimental results. The model presented in this study appears to be a useful tool for product design purposes.

Keywords: Engineered wood flooring, finite element modeling, dimensional stability, hygromechanical deformation, UF resin properties, moisture transfer.

[†] Member of SWST.

¹ Former Ph.D. candidate Département des sciences du bois et de la forêt, Université Laval Groupe interdisciplinaire de recherche en éléments finis (GIREF) Québec, Canada G1K 7P4

INTRODUCTION

Engineered wood flooring increases its global market share every year. Irland (1990) and Lamy (1997) noted that engineered wood flooring is increasingly popular in a context where hardwood flooring in general makes a remarkable comeback since the early eighties. The rapid growth in the wood flooring market share appears to be related mostly to the repair and remodeling sector and to the consumer's desire for a healthier indoor environment. The total shipments of engineered wood flooring have been growing at a faster rate than total flooring material footage area (Anonymous 1998; Irland 1990). Floor Covering Weekly (Anonymous 2000) reports that carpets are losing market share to wood products in the United States because homeowners are looking for healthier products. In 1999, hardwood represented 8% of the floor covering sales in the United States, of which 39% was engineered wood flooring (Anonymous 2000). In 2000, hardwood flooring maintained its sales level with 8.4% of the floor covering market, but engineered wood flooring raised its share of the wood segment to 48% (Anonymous 2001).

To maintain its position in the hardwood flooring market, the North American industry must develop new-engineered wood flooring design and help optimize the use of the wood resource. In wood products design, dimensional stability is of primary importance especially in the use of wood-layered composites where a small deformation can result in poor behavior. This is particularly true for appearance products such as parquet, flooring, cabinetry, and furniture components. Non-homogeneous adsorption and desorption of water vapor by the composite may induce cupping, and consequently decrease product value. For appearance products, a small deformation in the material can result in an undesirable performance. In this context, the design of stable engineered flooring is of primary importance for the end value of the composite.

There is limited literature available on engineered wood flooring mainly because most re-

search and development on those products have been performed by the industry with the result that publicly available knowledge on the behavior of this product is limited. Kubler and Lempius (1972) introduced the European technology used by this industry 30 years ago. Recent publications present work on the glue-line fatigue in engineered wood flooring (Blanchet et al. 2003a) and the behavior of various engineered wood flooring constructions (Blanchet et al. 2003b).

Numerical predicting tools such as the finite element method can be used to solve applied physical and mechanical laws and predict the behavior of engineered wood flooring (Reddy 1993; Cloutier et al. 2001). They can be helpful in providing direction in design and are expected to decrease testing time and cost. Gendron et al. (2004) have presented a numerical study of the hygro-mechanical deformation of two cardboard layups using the finite element method. A similar application for solid wood was presented by Tong and Suchsland (1993).

The objective of this paper is to present an application of the finite element method used to simulate the behavior of engineered wood flooring and to demonstrate its potential in design. First, the problem is described. Then, the mathematical model and its discretization are presented. In the last section, the model is applied to the study of an engineered flooring strip. The results are presented in the fourth section. Finally, some conclusions are presented in the last section of the paper.

MODELING APPROACH

Problem statement

The flooring strip considered in this study is a free-standing three-layer strip (Fig. 1). It is 65 mm wide, 14 mm thick, and 1000 mm long. The construction considered is a 4-mm-thick sugar maple plank as surface layer (SL), an 8-mm-thick white birch core layer (CL), and a 2-mm-thick yellow birch veneer as backing layer (BL). The core layer is made of 22-mm-wide sticks with 2-mm spacing. A UF resin film is used to bond the layers together.

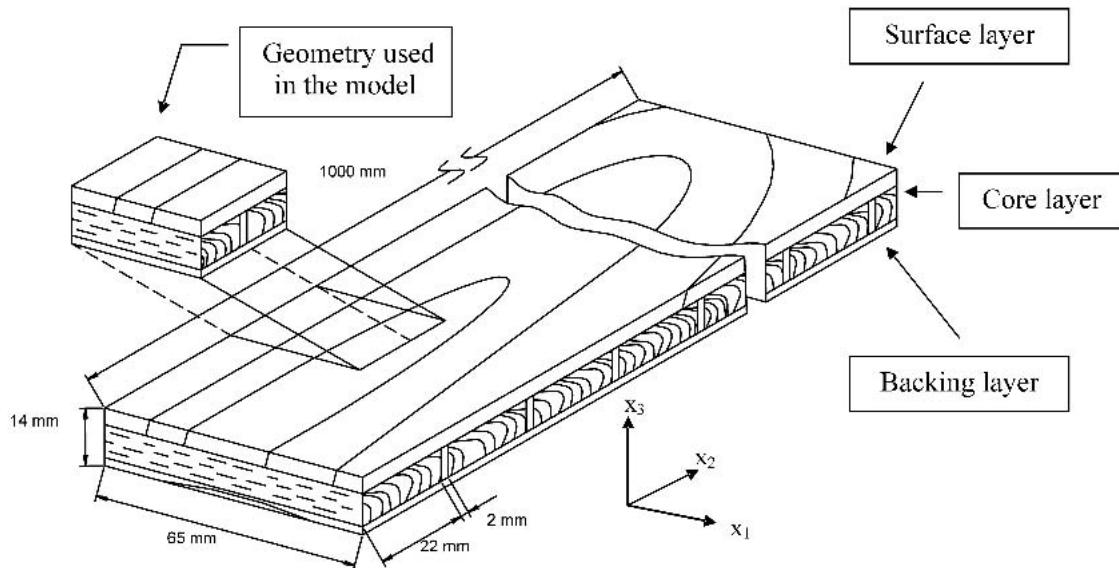


FIG. 1. Engineered wood flooring construction and the geometry used in the model.

The deformation is assumed to be caused by water vapor desorption from 6.3 to 5% occurring by convection from the top surface only. This corresponds to a decrease from 50 to 20% RH at 20°C. All other edges and the bottom surface are assumed impervious. Each wood layer of the composite is assumed orthotropic and elastic; no mechano-sorptive effects were taken into account as previous work demonstrated that the behavior is elastic under the conditions considered in this study (Blanchet et al. 2003b). Since the components were conditioned before and after assembly, the flooring is assumed to be initially free of stress.

Wood components properties

The modeling of the behavior of engineered flooring strips requires the knowledge of the physical and mechanical properties of the different wood species used for each layer as well as of the UF resin. The properties used in the current study are listed in Table 1. Some of them were taken from the literature and others were determined experimentally. The elastic and shear moduli as well as the Poisson's ratios of wood were obtained from Bodig and Jayne

(1993). The shrinkage and swelling coefficients of white and yellow birch were obtained from Jessome (2000). Sugar maple expansion coefficients were obtained from Goulet and Fortin (1975). The basic density, coefficients of contraction, as well as the elastic moduli of sugar maple were validated by laboratory experiments. The results obtained were similar to those presented by Bodig and Jayne (1993). The water vapor diffusion coefficients were taken from Siau (1995), except for the tangential and radial water vapor diffusion coefficients of sugar maple. In this case, the value in the radial direction was determined by the vapor cup method described by Siau (1995). This value was then used as the transverse water vapor diffusion coefficient for both the tangential and radial directions. The sugar maple water vapor diffusion coefficient is a semi-logarithmic function of the moisture content (Siau 1995); therefore, such relationship was used in the model to adjust the water vapor diffusion coefficient in the surface layer.

UF resin properties

A UF resin mix commonly found in industry was used in this study. This mix corresponds to

TABLE 1. Model parameters.

Parameter	Material			
	Surface	Core	Backing	Binder
	Sugar maple	White birch	Yellow birch	UF resin
d_b (kg m ⁻³)	¹ 597	¹ 559	¹ 506	⁴ 1500
D (m ² s ⁻¹)				⁶ 1.0×10^{-14}
D_L (m ² s ⁻¹)	² 1.3×10^{-8}	² 1.3×10^{-8}	² 1.3×10^{-8}	
D_R (m ² s ⁻¹)	⁵ 1.8×10^{-11}	² 4×10^{-11}	² 4×10^{-11}	
D_T (m ² s ⁻¹)	⁵ 1.8×10^{-11}	² 4×10^{-11}	² 4×10^{-11}	
M_0 (%)	8	8	8	6.3
M_∞ (%)	5	5	5	5
h (kg m ⁻² s ⁻¹ % ⁻¹)	² 3.2×10^{-4}	² 3.2×10^{-4}	² 3.2×10^{-4}	² 3.2×10^{-4}
$\beta_{\text{Laboratory}}$ (m m ⁻¹ % ⁻¹)				⁵ 1.9×10^{-3}
$\beta_{\text{Effective}}$ (m m ⁻¹ % ⁻¹)				⁵ 1.9×10^{-2}
β_L (m m ⁻¹ % ⁻¹)	⁷ 1.8×10^{-4}	¹ 1.5×10^{-4}	¹ 1.5×10^{-4}	
β_R (m m ⁻¹ % ⁻¹)	⁷ 1.9×10^{-3}	¹ 1.7×10^{-3}	¹ 1.9×10^{-3}	
β_T (m m ⁻¹ % ⁻¹)	⁷ 2.8×10^{-3}	¹ 2.4×10^{-3}	¹ 2.3×10^{-3}	
α_L (m m ⁻¹ % ⁻¹)	⁷ 1.5×10^{-4}			
α_R (m m ⁻¹ % ⁻¹)	⁷ 2.1×10^{-3}			
α_T (m m ⁻¹ % ⁻¹)	⁷ 3.3×10^{-3}			
E (Gpa)				⁴ 9
E_L (Gpa)	³ 13.810	³ 12.045	³ 15.251	
E_R (Gpa)	³ 1.311	³ 1.069	³ 1.251	
E_T (Gpa)	³ 0.678	³ 0.516	³ 0.641	
G_{LR} (GPa)	³ 1.013	³ 0.829	³ 0.971	
G_{RT} (GPa)	³ 0.255	³ 0.200	³ 0.242	
G_{LT} (GPa)	³ 0.753	³ 0.607	³ 0.721	
ν				⁴ 0.35
ν_{LT}	³ 0.50	³ 0.43	³ 0.45	
ν_{RT}	³ 0.82	³ 0.78	³ 0.70	
ν_{TL}	³ 0.025	³ 0.018	³ 0.018	
ν_{RL}	³ 0.044	³ 0.043	³ 0.035	
ν_{TR}	³ 0.42	³ 0.38	³ 0.36	
ν_{LR}	³ 0.46	³ 0.49	³ 0.43	

¹Jessome (2000), ²Siau (1995), ³Bodig and Jayne (1993), ⁴Dorlot et al. (1986), ⁵experimental value, ⁶estimated value, ⁷Goulet and Fortin (1975).

100 parts (weight or volume based) of UF resin, 2.5 parts of catalyst, 50 parts of wheat flour, 5 parts of nut shell flour, and 30 parts of water. The UF resin modulus of elasticity was obtained from Wellons (1981), and the Poisson's ratio was obtained from Dorlot et al. (1986).

The water vapor diffusion coefficient of the UF resin was too low to be measured by the vapor cup method even with an accurate balance (0.001 g). Therefore, an alternative technique was developed to determine both water vapor diffusion and expansion coefficients of the UF resin. A one-mm-thick UF film was obtained in a 300-mm by 300-mm press. The resin was pressed between two Teflon sheets, and the thickness of the film produced was controlled by

a one-mm-thick veneer strip. These films were cured for 1 h at 90°C at a pressure of 1300 kPa. The films were placed successively in two conditioning rooms at 20°C; the first one was set at 20% relative humidity (RH) and the second one at 80% RH. Moisture equilibrium was reached under these conditions. The reach of equilibrium was determined by weight. Moisture expansion coefficient was also determined during this experiment. To calculate the moisture expansion coefficient, the distance between two markers on the films was measured with a stereomicroscope assembled on a micrometric mobile table.

The time required to obtain the equilibrium was used to determine the water vapor diffusion coefficient using a finite element model simu-

lating the UF film. The in-plane dimensions of the finite element domain correspond to a quarter of the UF resin film tested in conditioning rooms (Fig. 2a). Symmetric boundary conditions were applied. The elements used in the model had the same thickness, width, and length as those used in the glue-line of the flooring model. As the UF resin films were free-standing, boundary conditions were established to reflect this situation.

Preliminary work has shown that the wood-UF resin interface has different properties in service than a free film of UF resin. Therefore, we defined the effective expansion coefficient as the expansion coefficient of the material in service. To obtain this value, we defined two more models (Fig. 2b and 2c). Figure 2b presents a first model that was used to model the in-plane swelling of a 1-mm-thick veneer. A second model (Fig. 2c) was used to model the in-plane swelling of a composite made of a 1-mm-thick veneer layer, a 0.01-mm-thick UF resin layer, and an-

other 1-mm-thick veneer layer (from top to bottom). Simulations were performed to reproduce corresponding experimental results obtained for the test set-ups shown in Fig. 2. Finite element meshes used for these models had similar density as for the flooring model (Fig. 3). The test specimens were submitted to the same temperature and relative humidity conditions as defined in the previous section until constant weight was reached.

Mathematical model

The governing equations used in the model are the three-dimensional equations of equilibrium given in Eq. (1):

$$\begin{aligned} \frac{\partial \sigma_1}{\partial x_1} + \frac{\partial \sigma_{12}}{\partial x_2} + \frac{\partial \sigma_{13}}{\partial x_3} &= 0 \\ \frac{\partial \sigma_{12}}{\partial x_1} + \frac{\partial \sigma_2}{\partial x_2} + \frac{\partial \sigma_{23}}{\partial x_3} &= 0 \\ \frac{\partial \sigma_{13}}{\partial x_1} + \frac{\partial \sigma_{23}}{\partial x_2} + \frac{\partial \sigma_3}{\partial x_3} &= 0 \end{aligned} \quad (1)$$

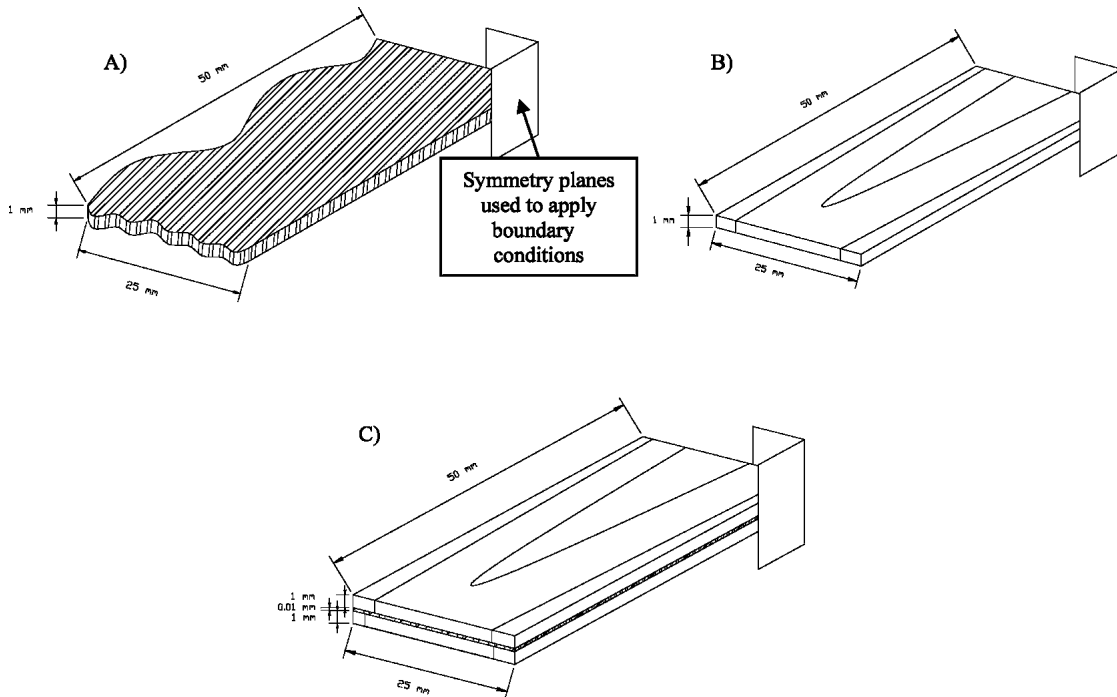


FIG. 2. Models used to determine the UF resin expansion and water vapor diffusion coefficients. A) UF resin film, B) Veneer and C) composite made of veneer, UF resin and veneer.

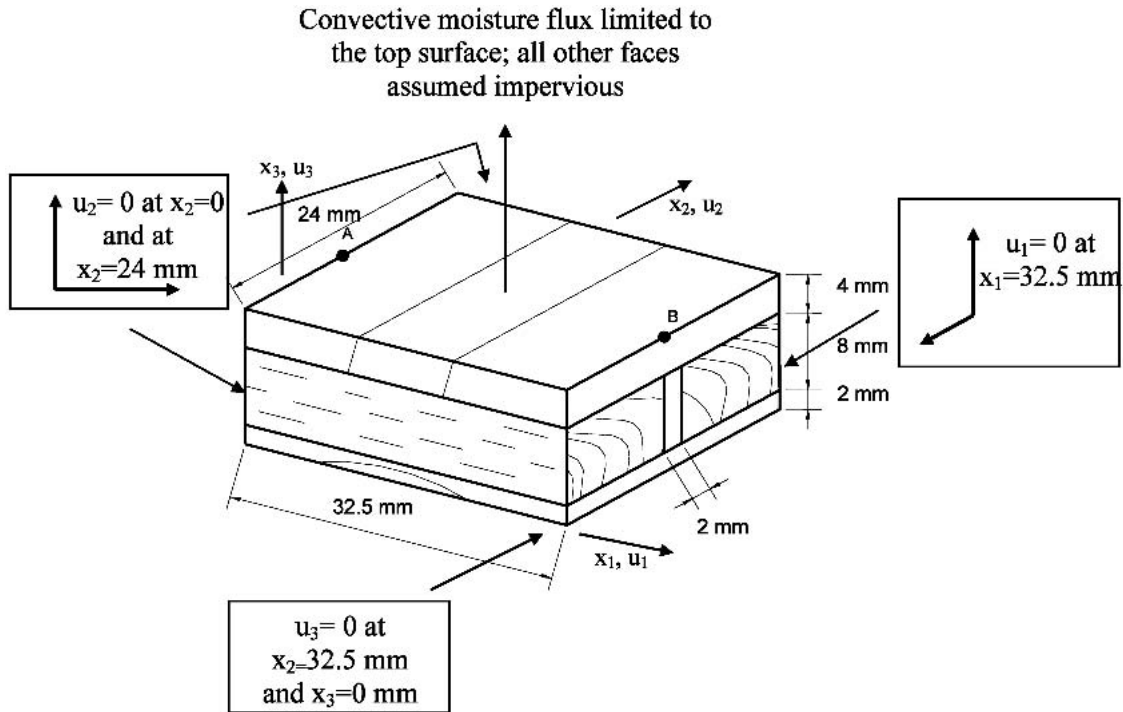


FIG. 3. Boundary conditions applied to the domain of the model and locations used to determine the cupping deformation.

where the body forces are assumed to be negligible. σ_1 , σ_2 , and σ_3 are the normal stress components, and σ_{12} , σ_{13} , and σ_{23} are the shear stress components expressed in the (x_1, x_2, x_3) rectangular coordinate system. It is assumed that the x_1 -, x_2 -, and x_3 - directions correspond to the

principal material directions of wood. Because the wood material and the UF resin are assumed elastic, Hooke's law is being used to relate stresses to strains (Bodig and Jayne 1993) in the following modified version as suggested by Tong and Suchsland (1993):

$$\begin{Bmatrix} \sigma_1 \\ \sigma_2 \\ \sigma_3 \\ \sigma_{23} \\ \sigma_{13} \\ \sigma_{12} \end{Bmatrix} = \begin{bmatrix} \frac{1 - \nu_{23}\nu_{32}}{E_2E_3S} & \frac{\nu_{21} + \nu_{23}\nu_{31}}{E_2E_3S} & \frac{\nu_{31} + \nu_{21}\nu_{32}}{E_2E_3S} & 0 & 0 & 0 \\ \frac{\nu_{21} + \nu_{23}\nu_{31}}{E_2E_3S} & \frac{1 - \nu_{31}\nu_{13}}{E_1E_3S} & \frac{\nu_{23} + \nu_{21}\nu_{13}}{E_1E_2S} & 0 & 0 & 0 \\ \frac{\nu_{31} + \nu_{21}\nu_{32}}{E_2E_3S} & \frac{\nu_{23} + \nu_{21}\nu_{13}}{E_1E_2S} & \frac{1 - \nu_{21}\nu_{12}}{E_1E_2S} & 0 & 0 & 0 \\ 0 & 0 & 0 & G_{23} & 0 & 0 \\ 0 & 0 & 0 & 0 & G_{13} & 0 \\ 0 & 0 & 0 & 0 & 0 & G_{12} \end{bmatrix} \begin{pmatrix} \begin{Bmatrix} \epsilon_1 \\ \epsilon_2 \\ \epsilon_3 \\ \gamma_{23} \\ \gamma_{13} \\ \gamma_{12} \end{Bmatrix} - \begin{Bmatrix} \beta_1\Delta M \\ \beta_2\Delta M \\ \beta_3\Delta M \\ 0 \\ 0 \\ 0 \end{Bmatrix} \end{pmatrix} \quad (2)$$

with

$$S = \frac{1}{E_1 E_2 E_3} (1 - 2\nu_{21}\nu_{32}\nu_{13} - \nu_{13}\nu_{31} - \nu_{23}\nu_{32} - \nu_{12}\nu_{21}) \quad (3)$$

where E_i : moduli of elasticity; G_{ij} : shear moduli; ν_{ij} : Poisson's ratios; ε_i : normal strain components; γ_{ij} : engineering shear strain components; β_i : moisture shrinkage/swelling coefficients ($\%^{-1}$); ΔM : moisture content change (%). Because the UF resin is assumed isotropic, Hooke's law can be simplified for that component of the composite by assuming: $E_1 = E_2 = E_3 = E$, $\nu_{23} = \nu_{32} = \nu_{13} = \nu_{31} = \nu_{12} = \nu_{21} = \nu$, $G_{23} = G_{13} = G_{12} = E/2(1 + \nu)$, $\beta_1 = \beta_2 = \beta_3 = \beta$.

Finally, the normal and shear strains are related to the displacements, u_1 , u_2 , and u_3 measured along the x_1 , x_2 , and x_3 directions, respectively, through the following relationships (Jones 1975):

$$\begin{aligned} \varepsilon_1 &= \frac{\partial u_1}{\partial x_1} & \gamma_{12} &= \frac{\partial u_1}{\partial x_2} + \frac{\partial u_2}{\partial x_1} \\ \varepsilon_2 &= \frac{\partial u_2}{\partial x_2} & \gamma_{13} &= \frac{\partial u_1}{\partial x_3} + \frac{\partial u_3}{\partial x_1} \\ \varepsilon_3 &= \frac{\partial u_3}{\partial x_3} & \gamma_{23} &= \frac{\partial u_2}{\partial x_3} + \frac{\partial u_3}{\partial x_2} \end{aligned} \quad (4)$$

The transient moisture movement through the model is governed by a three-dimensional conduction equation (Siau 1995) that can be written as follows:

$$\frac{d_b}{100} \frac{\partial M}{\partial t} - \left\{ \frac{\partial}{\partial x_1} \frac{\partial}{\partial x_2} \frac{\partial}{\partial x_3} \right\} \left[\begin{array}{ccc} \left(\begin{array}{ccc} K_{M11} & 0 & 0 \\ 0 & K_{M22} & 0 \\ 0 & 0 & K_{M33} \end{array} \right) \left\{ \begin{array}{c} \frac{\partial M}{\partial x_1} \\ \frac{\partial M}{\partial x_2} \\ \frac{\partial M}{\partial x_3} \end{array} \right\} \end{array} \right] = 0 \quad (5)$$

with

$$K_{Mii} = \frac{D_{ii} d_b}{100} \quad (6)$$

where M : moisture content (oven-dry basis) ($\text{kg kg}^{-1} \times 100$); t : time (s); K_{Mii} : components of the tensor of effective diffusivity ($\text{kg m}^{-1} \text{s}^{-1} \%^{-1}$); D_{ii} : components of the tensor of effective diffusion ($\text{m}^2 \text{s}^{-1}$); d_b : basic density (kg m^{-3}). Because the chosen coordinate system (x_1, x_2, x_3) coincides with the principal directions of wood, the tensor of effective diffusivity is diagonal. Also because UF resin is assumed isotropic, Eq. (6) is simplified in this case by assuming: $D_{11} = D_{22} = D_{33} = D$.

Discretization of the mathematical model

The finite element modeling of hygro-mechanical distortion of engineered wood flooring was performed using the pre- and post-processing software PATRAN and the finite element software ABAQUS. The finite element discretization of the Galerkin weak form of the equilibrium (1) and moisture transfer equations (5) is performed using standard isoparametric interpolation of the unknown displacements u_1 , u_2 , u_3 and M . Essential boundary conditions correspond to specified values of the displacements, u_1 , u_2 , and u_3 , or moisture content, M . Natural boundary conditions correspond to specified values of the normal stress vector or moisture flux. The time discretization of the equation is accomplished with the standard Euler implicit time marching scheme. The predicted values of M and u_1 , u_2 , and u_3 depend on the position as well as time. A single coupled system of discrete equations is solved for the displacements and M at each time step. A user-specified initial time increment of 1300 s is specified. It corresponded to the largest increment leading to a stable and convergent numerical solution. The following time increments are automatically adjusted by ABAQUS based on the convergence rate.

Application of the discretized model to engineered wood flooring

The proposed model was used to predict the deformation of the central part of an engineered wood flooring strip as shown in Fig. 1. The

model corresponds to half the width of the strip and a length of 24 mm. This length actually includes two half width core sticks (2×11 mm) and a 2-mm space between the sticks (Fig. 3). The length of the model geometry was small in regard to the total length of the validation strip (24 mm/1000 mm). Points A and B were located on nodes. The locations of these points were (0 mm, 11 mm, 14 mm) and (32.5 mm, 14 mm, 11 mm), respectively, as indicated on Fig. 3.

The principal material directions of wood are assumed perfectly oriented with the strip, and wood growth rings are assumed perfectly flat. As a result, a Cartesian coordinate system can be used. The tangential, axial, and radial properties of wood are specified for both the surface and the backing layers in the x_1 -, x_2 -, and x_3 -directions, respectively. In core layer x_1 -, x_2 -, and x_3 -directions correspond to axial, radial, and tangential wood directions, respectively as this layer is cross-grain-oriented compared to the surface and the backing layers. Wood properties are assumed constant, except for the sugar maple transverse water vapor diffusion coefficient, which varies according to the following equation $D_{ii} = 3.8 \times 10^{-12} M - 5.37 \times 10^{-12}$ (Siau 1995). The model does not consider any interface layer between the wood layers and the gluelines. The model assumes that the UF resin is as hygroscopic as wood. No fatigue has been considered in the glueline. Swelling and shrinkage hysteresis were taken into account using adsorption and desorption isotherm equations in the model. Sorption isotherms are from the results of Goulet and Fortin (1975).

The finite element mesh applied to the geometry is shown in Fig. 4. A total of 2864 hexahedral 8-node elements were used for the three layers of wood as well as for the two gluelines. Elements of the surface layer were 0.5 mm thick and core layer elements were one mm thick. Elements of the backing layer were 2 mm thick. Glueline elements were assumed to be 0.1 mm thick. Element dimensions in the x_1 and x_2 directions were approximately 2×2 mm.

Initial and boundary conditions must be specified for the moisture transfer as well as the me-

chanical part of the model. The initial condition corresponding to the moisture transfer part of the model, Eq. (7), specifies that the initial moisture content is constant at every point in the model.

$$M(x_1, x_2, x_3, t_0) = M_0 = 6.3\% \quad \forall(x_1, x_2, x_3) \quad (7)$$

The boundary conditions specify no moisture flux through any surface except the top one through which desorption is assumed to occur. Through the top air-wood interface, a convective mass transfer determined by the following equation is assumed:

$$q = h(M_s - M_\infty) \quad (8)$$

where h : convective mass transfer coefficient ($\text{kg m}^{-2} \text{s}^{-1} \%^{-1}$) (Siau 1995); M_s : surface moisture content (%); M_∞ : equilibrium moisture content (5%).

The following initial and boundary conditions were used for the mechanical part of the model. The initial conditions correspond to the fact that the flooring strip is initially assumed stress-free and undeformed. The initial conditions can be expressed as:

$$\sigma(x_1, x_2, x_3, t_0) = \sigma_0 = 0 \quad \forall(x_1, x_2, x_3) \quad (9)$$

$$u(x_1, x_2, x_3, t_0) = u_0 = 0 \quad \forall(x_1, x_2, x_3) \quad (10)$$

The essential boundary conditions are illustrated in Fig. 2. They are described by Eqs. (11) to (13).

$$u_1 = 0 \quad \text{at } (32.5, x_2, x_3) \text{ (mm)} \quad (11)$$

$$u_2 = 0 \quad \text{at } (x_1, 0, x_3) \text{ and } (x_1, 24, x_3) \text{ (mm)} \quad (12)$$

$$u_3 = 0 \quad \text{at } (32.5, x_2, 0) \text{ (mm)} \quad (13)$$

Equation (11) creates a symmetry axis along the centerline of the free-standing strip. Equation (12) specifies that the domain considered cannot elongate since it is part of a longer strip. This corresponds to the restraint that would be provided longitudinally by the remaining part of

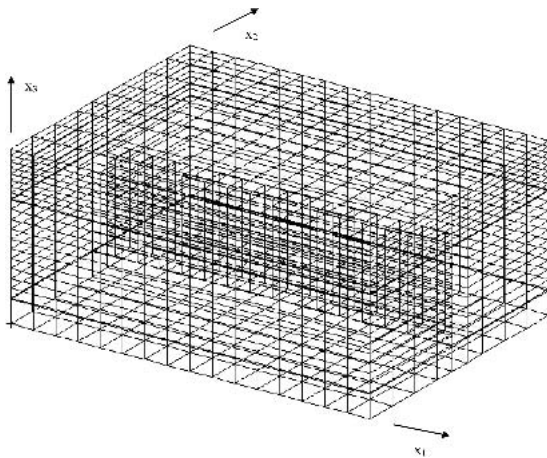


FIG. 4. Mesh used in this study.

the flooring strip which is not modeled. Equation (13) specifies that the bottom part of the strip can not move along the x_3 axis. This line becomes the reference line for the determination of points A and B, used to calculate the amplitude of the deformation.

Model validation

Experimental validation of the numerical results was performed. Prototypes were assembled with conditioned material (20°C, 50% RH) in a hot press with UF resin as binder. The prototypes were then conditioned at 20°C and 50% RH. These conditions led to a measured equilibrium moisture content of 6.3%. Ten 65-mm-wide, 14-mm-thick, and 1-m-long strips were sealed with silicone and aluminium foil on the bottom face and the edges to limit moisture desorption to the top surface. The prototypes were placed in a conditioning room at 20°C and 20% RH for 42 days. Distortion measurements were done at five marked locations on each strip with a dial gauge as described in Blanchet et al. (2003b) (Fig. 5).

RESULTS AND DISCUSSION

UF resin properties

The UF resin water vapor diffusion coefficient was found to be $1 \times 10^{-14} \text{ m}^2/\text{s}$, a value

three orders of magnitude (1000×) lower than for wood. This value gives equivalent moisture transfer equilibrium periods with both the modeling and experimental approaches described in the previous section.

The moisture expansion coefficient of the UF resin was experimentally determined as 0.0019 mm per mm for 1% moisture content variation for a free 1-mm-thick UF film. This value was used in the model described in Fig. 2c. The linear expansion obtained with this model was 25% higher than the experimental value for similar time periods to reach the equilibrium. Since the linear expansion coefficients obtained with the UF film model (Fig. 2a) and the wood veneer model (Fig. 2b) were within 5% of the experimental results, an interaction between wood and the UF resin was assumed to explain the model (Fig. 2c) overestimation. Iterative simulations were performed using different UF resin expansion coefficients to reach the same linear expansion coefficient as the one obtained experimentally (Fig. 2c). An effective UF resin coefficient of 0.019 mm per mm was determined. This value was then used in the flooring models. This approach was also used by Triche (1988) to define material properties to be used in a finite element model.

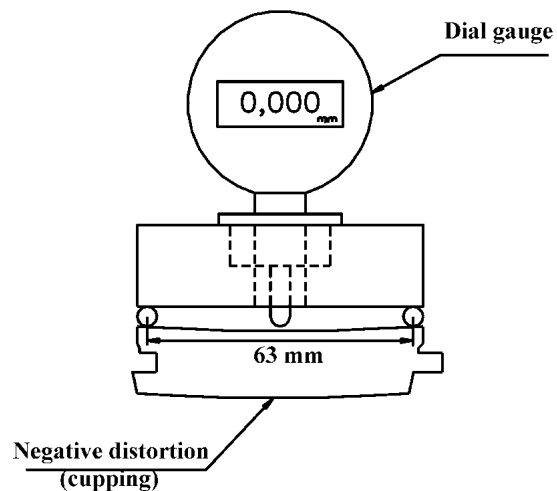


FIG. 5. Experimental determination of the cupping deformation.

Model predictions and experimental validation

Figure 6 presents the conditions recorded every 3 min in the conditioning room during the experiment. It can be seen that the conditions were not perfectly stable. Temperature increases and relative humidity drops illustrated in Fig. 6 resulted from the opening of the conditioning room door for each measurement. In Fig. 6, although the temperature is quite stable, the relative humidity keeps decreasing slowly as time unfolds. Similar but simplified conditions were used for the simulation as shown in Fig. 7. Conditions that result in less than 0.05% variation of wood equilibrium moisture content were grouped to reduce the calculation time. The variation in the room conditions resulted in the occurrence of both adsorption and desorption of moisture during the experiment. These variations are taken into account in the model.

Figure 8 presents the predicted and observed difference between the vertical displacement, u_3 ,

of points A and B of engineered wood flooring strips (see Fig. 3) as a function of time. Simulated and experimental curves are in reasonable agreement. Also, parametric studies have shown that during the first 3 days of conditioning, the slope of the curve is strongly influenced by the value of the transverse water vapor diffusion coefficient of the surface layer. Later during the experiment, the moisture reaches the glue line, and the deformation curve turns into a plateau. The rate of drying is then controlled by the UF resin water vapor diffusion coefficient. In the present case, the plateau is not perfect as the room relative humidity conditions (Figs. 6 and 7) were getting slightly more severe along the conditioning period. Simulations in stable conditions were generated, and a perfect plateau in the curve of cupping as a function of time was obtained. Approximately 83% of the maximum distortion occurs within the first 10 days of the experiment. The model overestimates the maxi-

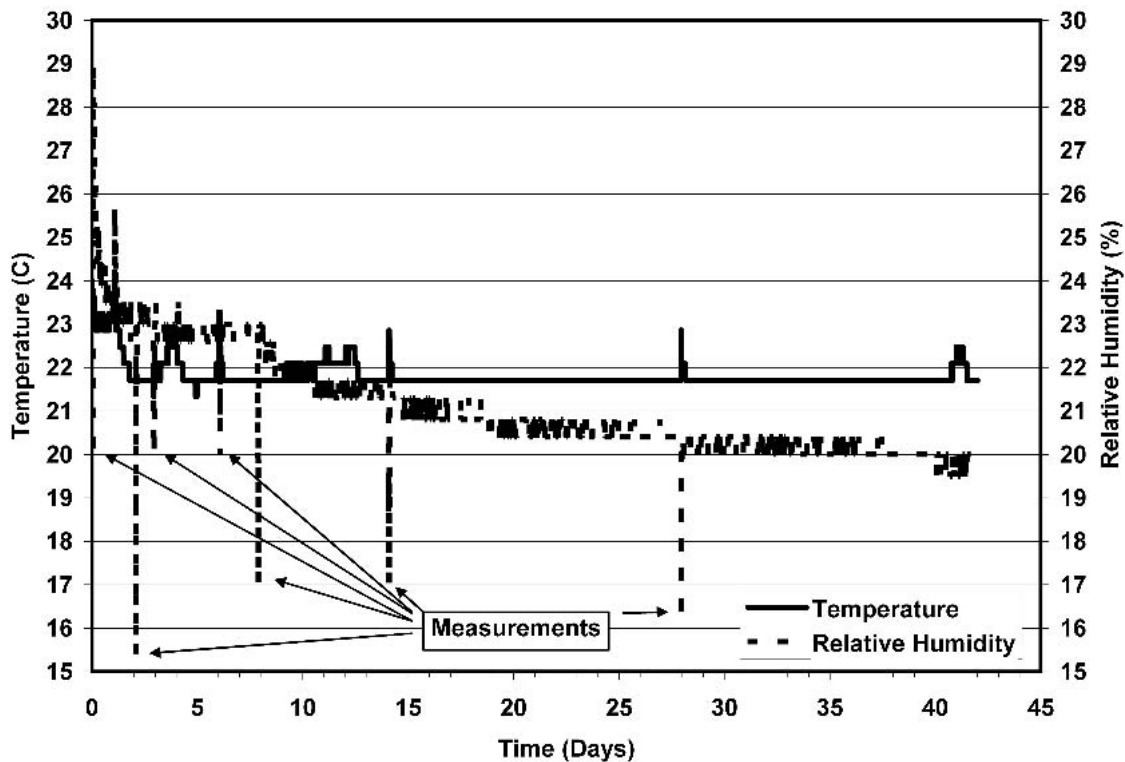


FIG. 6. Room conditions.

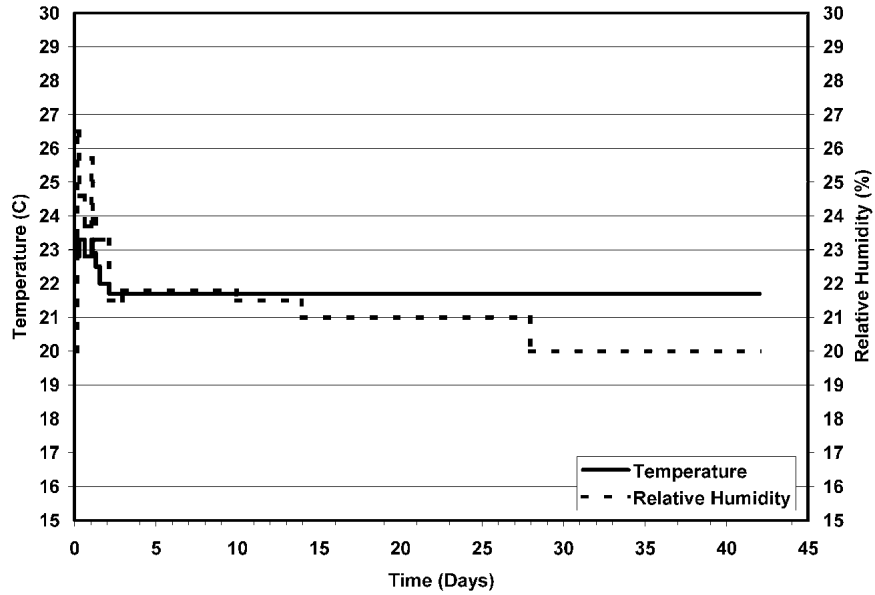


FIG. 7. Conditions used to approximate the experimental room conditions.

imum distortion by approximately 12%. However, the predicted results are within the standard deviation of the experimental results.

Figure 9 shows the predicted moisture distri-

butions corresponding to four different time values. The results illustrate the effect of the glue-line between the surface layer and the core layer on the moisture profile for engineered flooring

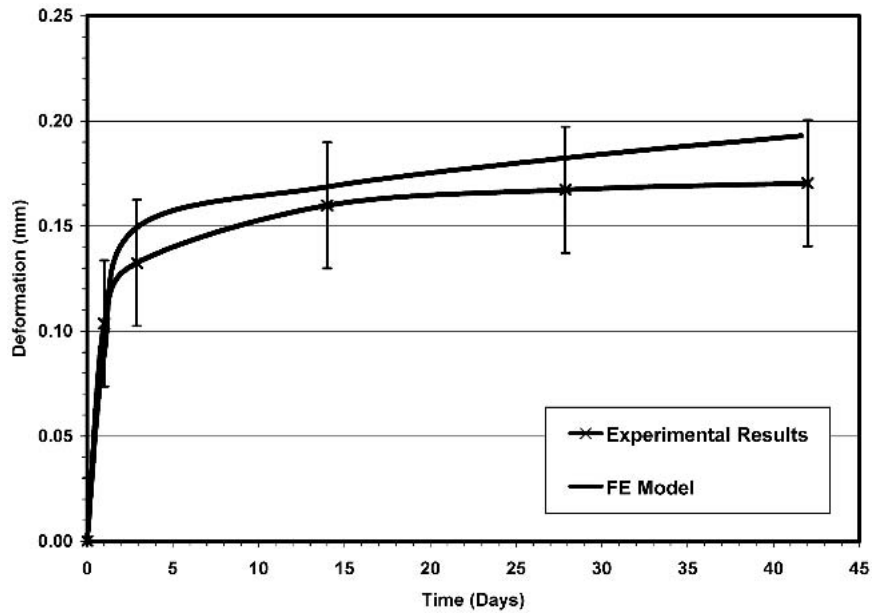


FIG. 8. Predicted and observed cupping deformation as a function of time. Error bars are the standard deviation observed in the experiment. (The cupping deformation corresponds to the difference between the vertical displacement, u_3 , of points A and B shown in Fig. 2)

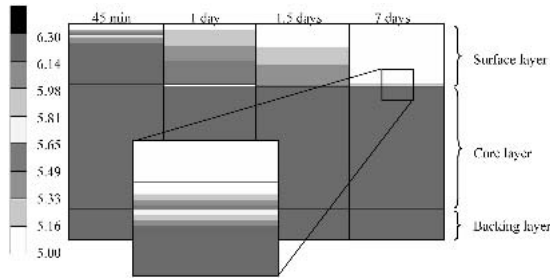


FIG. 9. Predicted moisture distribution across the thickness of the strip at four time values.

strips. Early during the simulation, the moisture gradient is established at the top surface of the sugar maple layer. Then, the glueline acts as a water vapor barrier and holds the drying front at the interface of the surface layer and the glueline (Fig. 9). That maintains the cupping deformation almost constant as the core, and the backing layers are still in their undeformed shape and the surface layer has shrunk significantly. This is the consequence of a lower water vapor diffusion coefficient in UF resin than in wood resulting in the surface layer reaching the 5% moisture content equilibrium while the subsequent layers are still close to their initial moisture content. Figure 9 illustrates the moisture trapped at the top wood-glue interface that is responsible for the plateau in the curves of Fig. 8. The level of this plateau is determined by the UF resin coefficient of moisture expansion.

CONCLUSIONS

Experimental results demonstrate that the finite element modeling approach can be used to predict the deformation of engineered wood flooring strips subjected to non-homogeneous moisture transfer. After 3 days of conditioning, 80% of the cupping deformation had appeared in the experiment. For predicted deformation, 78% of the cupping deformation appears after 3 days of conditioning. After 42 days of conditioning, the model results had overestimated the experiment results by 12% but were within the standard deviation of the experimental results.

The results of this study demonstrate that the

glueline between the surface layer and the core layer has an important contribution in the composite behavior. Layered wood flooring strips develop cupping deformation and maintain it due to the shrinkage of the surface, while the core and backing layers do not change dimensions. This behavior is explained by the low water vapor diffusion coefficient of the gluelines, especially the one between the surface and core layers.

The model presented in this study appears to be a useful tool for design purposes. Different materials and geometries can be assessed to investigate different strip constructions. Future work will include the modeling of the impact of a varnish layer applied to the top surface on the strip behavior. Also, it may be of interest to investigate UF resin properties in more details in the future given its importance in the behavior of the composite.

ACKNOWLEDGMENTS

The authors wish to thank the Fonds de recherche sur la nature et les technologies (FQRNT fund) under its industry-university program, the NSERC Industrial Chair on Engineered Wood Products for Structural and Appearance Applications, the NSERC Research Grant no. 121954 and Forintek Canada Corp. for their financial support.

REFERENCES

- ANONYMOUS. 1998. Worldwide Parquet Market Outlook. 2nd ed., RWS-Engineering Oy, Lahti, Finland. 171 pp.
- . 2000. Statistical report '99, Floor Covering Weekly, Vol. 47, No. 19, Garden City, NJ.
- . 2001. Statistical report '00, Floor Covering Weekly, Vol. 50, No. 18, Garden City, NJ.
- BLANCHET, P., R. BEAUREGARD, A. ERB, AND M. LEFEBVRE. 2003a. Comparative study of four adhesives used as binder in engineered wood parquet flooring. *Forest Prod. J.* 53(1):89–93.
- , ———, A. Cloutier, and G. Gendron. 2003b. Evaluation of various engineered wood parquet flooring constructions. *Forest Prod. J.* 53(5):30–37.
- BODIG, J., AND B.A. JAYNE 1993. *Mechanics of wood and wood composites*. Krieger Publishing Company, Malabar, FL. 712 pp.

- CLOUTIER, A., G. GENDRON, P. BLANCHET, S. GANEV, AND R. BEAUREGARD. 2001. Finite element modeling of dimensional stability in layered wood composites. Pages 63–72 in M. P. Wolcott, ed. Proc. 35th International Particle-board/Composite Materials Symposium, Washington State University, April 3–5. Pullman, WA.
- DORLOT, J.-M., J.-P. BAILON, AND J. MASOUNAVE. 1986. Des Matériaux. [Materials. (in French)] 2nd ed., École Polytechnique de Montreal editor. 467 pp.
- GENDRON, G., M. L. DANO, AND A. CLOUTIER. 2004. A numerical study of hygro-mechanical deformation of two cardboard layups. *Composites Sci. Technol.* 64: 619–627.
- GOULET, M., AND Y. FORTIN. 1975. Mesures du gonflement de l'érable à sucre au cours d'un cycle de sorption d'humidité à 21°C. [Swelling measurement in sugar maple in a soption cycle at 21°C. (in French)] Research note No. 12. Département d'exploitation et utilisation des bois. Université Laval, Quebec, Canada. 49 pp.
- IRLAND, L. C. 1990. The market for hardwood flooring: Conditions, competition, trends, and implication for Pennsylvania producers. Penn. Hardwoods Development Council, Technical Publication No.1, S. B. Jones and J. A. Stanturf Series eds. PA. 42 pp.
- JESSOME, A. P. 2000. Strength and related properties of woods grown in Canada. Forintek Canada Corp. Special Publication SP514E. 37 pp.
- JONES, M. J. 1975. Mechanics of composite materials. Hemisphere Publishing Corporation, New York, NY. 344 pp.
- KUBLER, H., AND J. LEMPELIUS. 1972. Germany's parquet flooring industry – The struggle to survive. *Forest Prod. J.* 22(10):14–16.
- LAMY, C. 1997. Planchers de Bois Franc, tendances récentes sur les marchés américain, canadien et québécois. [Wood Flooring; Recent trends of American, Canadian and Quebec markets (in French)]. Ministère des Ressources naturelles du Québec. Québec, Canada, 103 pp.
- REDDY, J. N. 1993. An introduction to the finite element method. 2nd ed. McGraw Hill, New York, NY. 684 pp.
- SIAU, J. F. 1995. Wood: Influence of moisture on physical properties. Department of Wood Science and Forest Products, Virginia Polytechnic Institute and State University, VA, Blacksburg, VA. 227 pp.
- TONG, Y., AND O. SUCHSLAND. 1993. Application of finite element analysis to panel warping. *Holz Roh- Werkst.* 51(1):55–57.
- TRICHE, M. H. 1988. Finite element modeling of a parallel aligned wood strand composite. Doctoral dissertation. Purdue University, Lafayette, IN.
- WELLONS, J. D. 1981. The adherents and their preparation for bonding. Pages 87–134 in Adhesive bonding of wood and other structural materials. Forest Products Laboratory, Forest Service, USDA and University of Wisconsin. A publication of the Educational Modules for Materials Science and Engineering (EMMSE) Project. Material Research Laboratory, The Pennsylvania State University. University Park, PA.